ACTA ASTRONOMICA
Vol. **80** (2020) pp. 1–9

A new mass determination of an eclipsing binary V2080 Cygni[1]

W. Dimitrov[1], K. Kamiński[1], K. Bąkowska[2],
M. K. Kamińska[1], J. Tokarek[1], M. Pawłowski[1], P. Bartczak[1]
T. Kwiatkowski[1], A. Schwarzenberg–Czerny[3]

[1] Astronomical Observatory Institute, Faculty of Physics,
Adam Mickiewicz University, ul. Słoneczna 36, 60-286 Poznań, Poland
e-mail: dimitrov@amu.edu.pl
[2] Institute of Astronomy, Faculty of Physics, Astronomy and Informatics,
Nicolaus Copernicus University, ul. Grudziądzka 5, 87-100 Toruń, Poland
[3] Nicolaus Copernicus Astronomical Center, ul. Bartycka 18, 00-716 Warsaw, Poland

Received January 30, 2021

ABSTRACT

We present new spectroscopic measurements of the eclipsing binary V2080 Cygni. It is a detached system with similar components and period of 4.9 d. We collected data with two instruments, 1.88 m DDO telescope equipped with Cassegrain spectrograph and 0.5 m PST1 connected to a fiber fed echellé spectrograph. We collected 127 measurements for each component, which significantly increase the number of available radial velocity measurements for the V2080 Cygni system. Obtained masses of the eclipsing components are $M_1 = 1.190 \pm 0.006$ and $M_2 = 1.139 \pm 0.005$ $M_\odot$. We compared both our data sets with the results of three other investigations. We also checked the influence of the usage of different measurement techniques: the cross-correlation and the Broadening Function method. We found that the obtained masses depend on the instrument used or measurment technique in about 1-2%, i.e. this is the level of the systematic errors that we could expect. Additionally, we analysed the GAIA mission results. V2080 Cygni A has three visual companions, however according to GAIA parallaxes and proper motions, they cannot be dynamically connected with the eclipsing binary and therefore are background stars. The possible existence of third body in the system could be cause of light-time effect. We collected multicolor photometry and calculated new times of minima. The $O-C$ diagrams indicate variation, which requires more recent data in order to be confirmed.

Key words: *Stars: individual: V2080 Cygni - binaries: eclipsing*

1. Introduction

Detached eclipsing binaries provide precise determination of stellar radii and masses. Modern photometric and spectroscopic observations allow us to reach the

[1] Based on the spectroscopic data obtained with Poznań Spectroscopic Telescope 1 and David Dunlap Observatory 1.88 m telescope.

accuracy of about 1% or better for those absolute parameters. The investigated star V2080 Cygni is a relatively bright F5 eclipsing binary with a visual magnitude of 7.4. Other designations of the object are HD 183361 and BD+49 3012. The object is listed as a visually multiple star in Catalog of the Components of Double and Multiple Stars (CCDM; Dommagnet & Nys 1994) and Washington Double Star Catalog (WDS; Mason et al. 2001). The eclipsing nature of the main A star was detected by Hipparcos satellite mission. The light curve has flat maxima and minima with comparable depth, as can be expected for similar, almost spherical components. The object is relatively bright and close, i.e. it is a good candidate for precise determination of absolute parameters. Spectral lines of both V2080 Cygni components are clearly seen. First radial velocity measurements were presented in a short IBVS paper (Kurpinska-Winiarska et al. 2000). Authors provided the amplitudes of radial velocity curves. They corrected the orbital period of the star, which is twice as long as the one given by Hipparcos. Later two teams observed the star spectroscopically. The first group collected 13 spectra at TUBITAK National Observatory and Catania Astrophysical Observatory (İbanoğlu et al. 2008). The velocities were measured with the cross-correlation method. The authors also observed the star photometrically and acquired UBV light curves. They obtained a model of the system using the Wilson-Devinney method. Authors mentioned the existence of third light in the system of about 3%. The second team obtained 8 spectra with the ELODIE spectrograph (Aliçavuş et al. 2019). For analysis they used the spectral disentangling method. Atmospheric parameters were obtained as well. For modelling of the star authors also used earlier radial velocity measurements of the first team and SuperWASP light curve. Authors detected third light of about 8% in both light curve modelling and spectrum disentangling. The results for masses from both studies agree within errors. The mass ratio is close to 1 and the obtained masses are 1.197 ± 0.005 $M_\odot$ for the primary component and 1.173 ± 0.004 $M_\odot$ for the secondary.

2. Visual companions

As was mentioned in the introduction, V2080 Cyg A has three bright visual companions. They are listed in WDS and CCDM catalogs of visual doubles. The latest results coming from GAIA mission[2] yield the parallaxes and the proper motions of all four components (Gaia Collaboration et al. 2016; Lindgren et al. 2016). GAIA DR2 results are presented in Table 1. Both DR1 and DR2 results are in good agreement and show that the all components have different parallaxes and proper motions and they are not connected dynamically. The fainter stars in the close neighbourhood also seem to be background stars, their proper motions and parallaxes are small (Fig. 1).

[2]https://gea.esac.esa.int/archive/

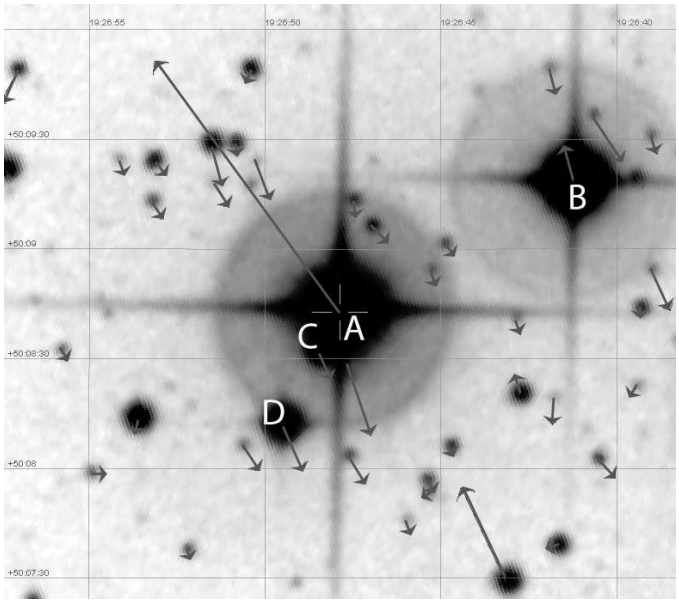

Fig. 1. Proper motions of V2080 Cyg A neighbourhood stars (GAIA DR2).

T a b l e 1

Proper motions and parallax for V2080 Cyg A and its potential companions from GAIA DR2 catalogue.

comp. WDS	phot. g (mag)	sep. (arcsec)	μ_α (mas/yr)	μ_δ (mas/yr)	parallax (mas)
A	7.24	-	55.50 ± 0.07	75.01 ± 0.07	11.70 ± 0.03
C	14.08	14	-2.97 ± 0.04	-5.94 ± 0.04	0.48 ± 0.03
D	11.49	36	-6.21 ± 0.06	-13.51 ± 0.05	0.57 ± 0.03
B	8.57	73	2.36 ± 0.13	10.41 ± 0.11	2.55 ± 0.05

3. Spectroscopy and measurements

Each of the two spectroscopic data sets used in the present study has been obtained with a different instrument. Both was analysed independantly and compared with each other, as well as with the data from the literature. Our spectroscopic observations complement the existing data and increase fhe number of all available observations in about four times.

The first data set was obtained with 1.88 m telescope of the David Dunlap Observatory with the Cassegrain spectrograph between April 21^{st} and November 10^{th} 2006. Two different detectors were used 1024x1024 Thomson CCD, and

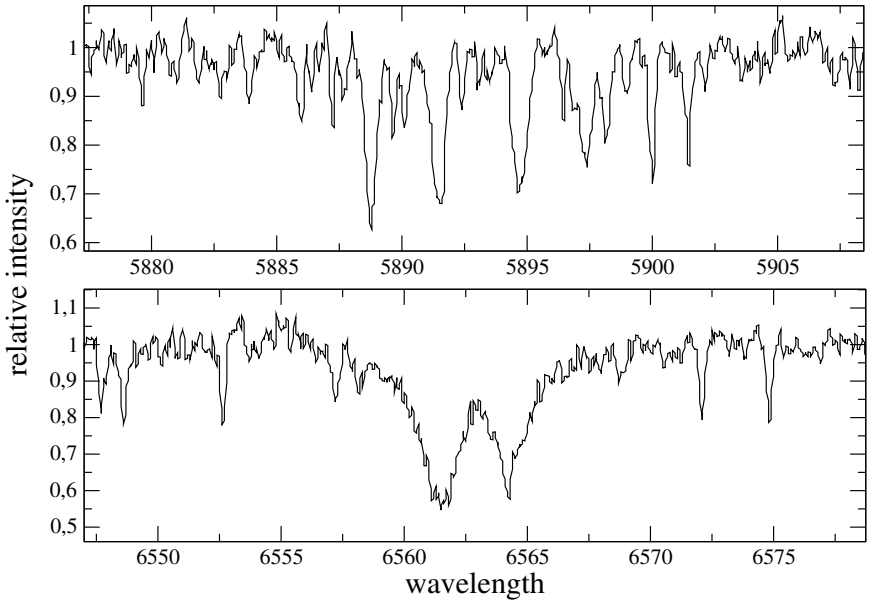

Fig. 2. Two spectral regions of a PST 1 spectrum: near NaD (top) and H_α (bottom) lines.

later 2048x512 Jobin Yvon Horiba CCD. The exposure times were 1200 s, and we observed the Mg spectral region near 5184 Å. The typical signal–to–noise ratio was in the range of 100 – 150. Data reduction was carried out using standard IRAF tasks.

The second dataset was acquired with 0.5 m Poznan Spectrocopic Telescope (PST1) between June 16^{th} and October 14th 2007. This instrument is smaller than the previous one, however it is connected via fiber to an echellé spectrograph (Baranowski et al. 2009). The system has very small light losses, as the telescope parameters fit perfectly the fiber requirements. The spectrograph is equipped with Andor DZ 436 CCD with 5 stage peltier plus liquid cooling. The spectral range was 4500 - 9200 Å with dispersion of 0.11 Å/pix. The exposure times were 1200 or 1800 s and the typical signal–to–noise ratio is 25–125. Two spectral regions are presented in Fig 2. The split spectral lines of both components are clearly seen.

We searched for traces of the third star, mentioned by the previous authors, in the cross correlation function. To enhance the signature of this component we used low temperature templates. We have not found any significant traces (Fig 3.).

For radial velocity measurements we have used the Broadening Function[3] (BF) method and for comparison and tests we also used the cross correlation (CCF) method. Broadening Function was first described by S. Rucinski (1992, 2002). The method is resistant to the spectral line broadening and has higher resolution compared to CCF. Typical BF for V2080 Cygni spectra is presented in Fig. 4. The

[3]http://www.astro.utoronto.ca/ rucinski/SVDcookbook.html

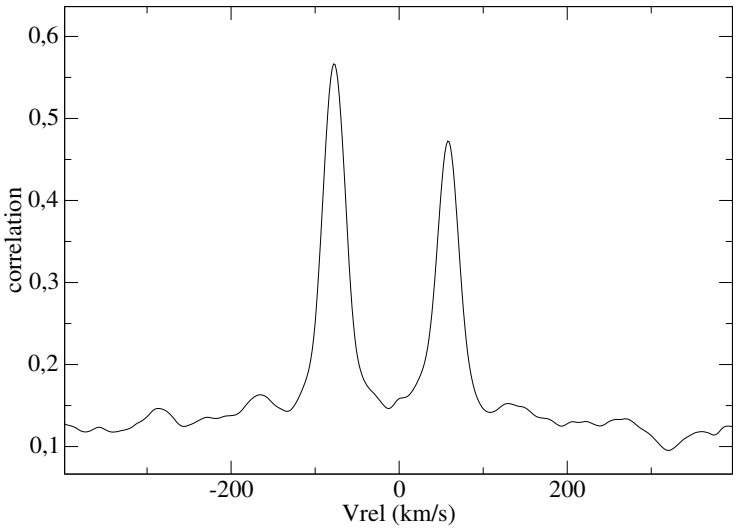

Fig. 3. Cross correlation function for PST 1 spectrum.

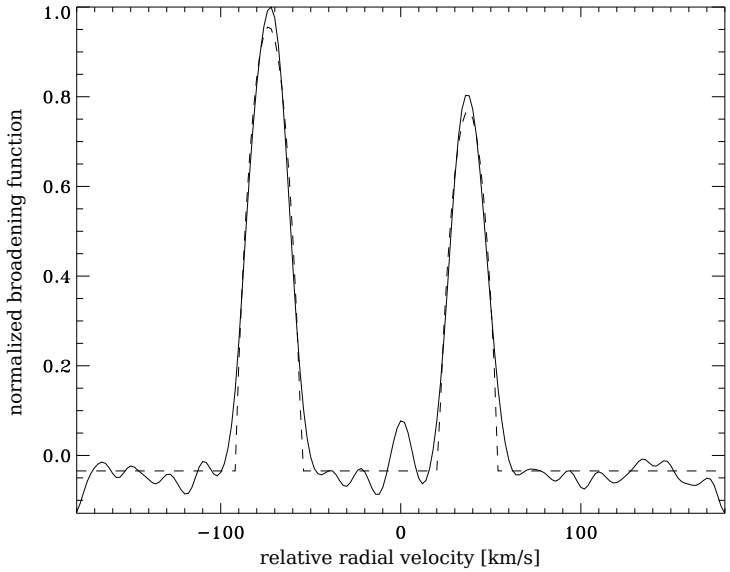

Fig. 4. Broadening function for one of the PST1 spectra. Solid line represents the BF and dashed line the fitted rotational profiles. The BF is normalized to 1. The horizontal axis represents the relative radial velocity. The third peak, near 0, is probably related to the telluric lines.

cross correlation measurements were carried out with IRAF task FXCOR.

4. Mass determination

For fitting of the radial velocity curves we have employed the PHOEBE SVN code (Prša & Zwitter 2005). The program is based on the Wilson-Devinney method (Wilson & Devinney 1971). As the results of the previous investigations sugest that the eclipsing pair could have a companion, we fitted the two data sets separately. For our fit we used the period of 4.933588(28) d given by İbanoğlu et al. (2008) and surface potentials and inclination presented by Aliçavuş et al. (2019). We fitted four parameters: semi-major axis, mass ratio, systemic velocity and HJD_0. HJD_0 was selected in the middle of the time span of RV observations. As there is a potential third body in the system we could expect light-time effect and possible phase shifts with respect to the ephemeris. That was the reason to leave this parameter free. The systemic velocity shows some variation that are slightly higher than what could be expected from zero point shifts in different spectrographs. It could be explained with the existence of third body and system's motion on the wide orbit.

First two columns of Table 2 present the influence of the usage of different instruments on the obtained results. In both cases Broadening Function method was used for the measurements. We compared data from 1.88 m DDO telescope and 0.5 m PST1 telescope. The signal-to-noise ratio of the DDO spectra is higher, however the PST1 echellé has a wider spectral range. The dispersion of the RV measurements for PST1 is smaller as can be expected for the spectrograph mounted in a thermally stabilized room. The measured semi-major axis of V2080 Cygni is in very good agreement, but the mass ratio differs by about 1%, which propagates into 1% differences in masses.

The second and third column of Table 2 show the same PST1 data set measured with two methods – BF and CCF. The mass ratio is in very good agreement, but the semi-major axis is slightly lower for the CCF results and that causes less than 1% lower masses.

The modern radial velocity measurements yield mass meaurements of eclipsing binaries with precision below 1%, however, as can be seen in the Table 2 and 3 results, masses could differ by about 1-2% depending on the instrument or measurement method used. Usually the listed errors of obtained parameters are based on the dispersion of the RV/LC measurements and do not take into account possible systematic errors.

4.1. Simultaneous fit

In this section we present the simultaneous fit for all our spectroscopic data. To achieve this we shifted up the first data set (DDO) by 1.1 $km\ s^{-1}$. This is the difference between the systemic velocities for both data sets. We compared the results with three other investigations (Table 3). Most of the results are in good agreement, only the systemic velocity values vary significantly. The masses for our result were calculated for the inclination of $86.^{\circ}009$ provided by Aliçavuş et al. (2019). The İbanoğlu et al. (2008) results were calculated for the inclination of

T a b l e 2

Comparison of BF and CCF fitting results for V2080 Cygni parameters based on our spectroscopic observations.

Instrument	DDO	PST1	PST1
Method	BF	BF	CCF
a ($R_\odot$)	16.16 ± 0.02	16.15 ± 0.02	16.12 ± 0.02
q	0.953 ± 0.003	0.965 ± 0.002	0.964 ± 0.002
V_γ (km s^{-1})	1.76 ± 0.09	2.86 ± 0.06	2.65 ± 0.06
$HJD_0 - 2450000$	3944.7883 ± 0.0012	4329.6078 ± 0.0008	4329.6072 ± 0.0008
M_1 ($M_\odot$)	1.193 ± 0.006	1.183 ± 0.006	1.177 ± 0.006
M_2 ($M_\odot$)	1.137 ± 0.006	1.142 ± 0.005	1.135 ± 0.005
σ_{RV} (km s^{-1})	1.08	0.59	0.57
n_{obs}	80	47	47

$86.^\circ 20$, which is very close to the upper one, therefore the results could be directly compared without recalculation of semi-major axes and masses. The earliest paper (Kurpińska-Winiarska et al. 2000) did not present neither inclination nor semi-major axis values. The error bars were not presented as well. To compare those results with most recent literature, we calculated the rest of the values using $i = 86.^\circ 009$.

All our moments of main eclipse, or HJD_0, (Table 2 and 3) were fitted to our RV data for the middle of the period of observation for each data set. The HJD_0 given by Kurpińska-Winiarska et al. (2000) is based on their radial velocity and photometric observations (Tab. 3). In the case of the İbanoğlu et al. (2008), result listed in Table 3, the HJD_0 value presents their best observed moment of the eclipse. The latest paper, K. Aliçavuş & Aliçavuş (2019), presents a value based on their RV data.

We collected four times more measurements than all the previous investigations together. Our primary mass value is close to the one obtained by İbanoğlu et al. (2008), while the secondary is about 2% lower. Mases obtained by Aliçavuş et al. (2019) are the highest among all results. Our result yields the lowest value of the mass ratio of the eclipsing pair.

Comparing the error bars of our and Aliçavuş et al. (2019) results listed in Table 3, we could mention that the authors have slightly smaller estimations of the errors. It is surprising because the quality of the RV data is comparable in both cases, while our analysis was carried out using six times more spectra. One significant difference between our and Aliçavuş et al. (2019) results is that we only fitted RV data and they made a simultaneous fit of RV and LC data. We performed

T a b l e 3

Comparison of V2080 Cygni parameters obtained in this work with values from the literature.

	Kurpińska-Winiarska et al. 2000	İbanoğlu et al. 2008	K. Aliçavuş & Aliçavuş 2019	PST1 & DDO (this paper)	bootst. err.
a ($R_\odot$)	16.16	16.20 ± 0.07	16.254 ± 0.019	16.16 ± 0.02	0.026
q	0.974	0.971 ± 0.009	0.982 ± 0.002	0.957 ± 0.002	0.002
V_γ (km s^{-1})	3.2	1.0 ± 0.4	1.17 ± 0.32	2.88 ± 0.06	0.08
HJD_0	1053.705	3895.4534	2504.186	4117.4638	
-2450000	± 0.001	± 0.0008	–	± 0.0009	0.0011
M_1 ($M_\odot$)	1.180	1.191 ± 0.017	1.197 ± 0.005	1.190 ± 0.006	0.007
M_2 ($M_\odot$)	1.149	1.157 ± 0.017	1.173 ± 0.004	1.139 ± 0.005	0.007
n_{obs}	11	13	21	127	
method	-	CCF	CCF	BF	

one of the bootstrap method variants to check our error estimations. We randomly draw N measurements from N observations with possible value repetitions. This way we obtained ten data sets for both components, and fitted RV_{12} curves. We calculated the standard deviation of obtained values of the parameters. Our formal errors listed in one before last column of Table 3 are in good agreement and slightly lower than the bootstrap errors listed in the last column.

5. Photometry

5.1. Observations and data reduction

Observations of V2080 Cyg were obtained during 41 nights between September 7^{th} to October 1^{st} 2011 at the Poznań Astronomical Observatory located in Poland. For observations we used a 200 mm, F/4.5 Newton reflector, equipped with SBIG ST-7 XME camera and a set of Bessel BVRI filters. The camera provided $17.0' \times 25.5'$ field of view.

All observations were carried out in the V, I and R filters with the exposure times of 10, 8 and 6 seconds, respectively. In total, we obtained 50699 exposures of V2080 Cyg during 108.59 hours. Table 4 presents a full journal of our CCD observations.

We determined relative unfiltered magnitudes of V2080 Cyg by taking the difference between the magnitude of the object and the mean magnitude of three comparison stars. In Fig. 6 the sky region is displayed with V2080 Cygni marked as V1 and the comparison stars as C1, C2 and C3, respectively. The equatorial coordinates and the brightness of comparison stars C1 (RA$= 19^h26^m41^s.246$,

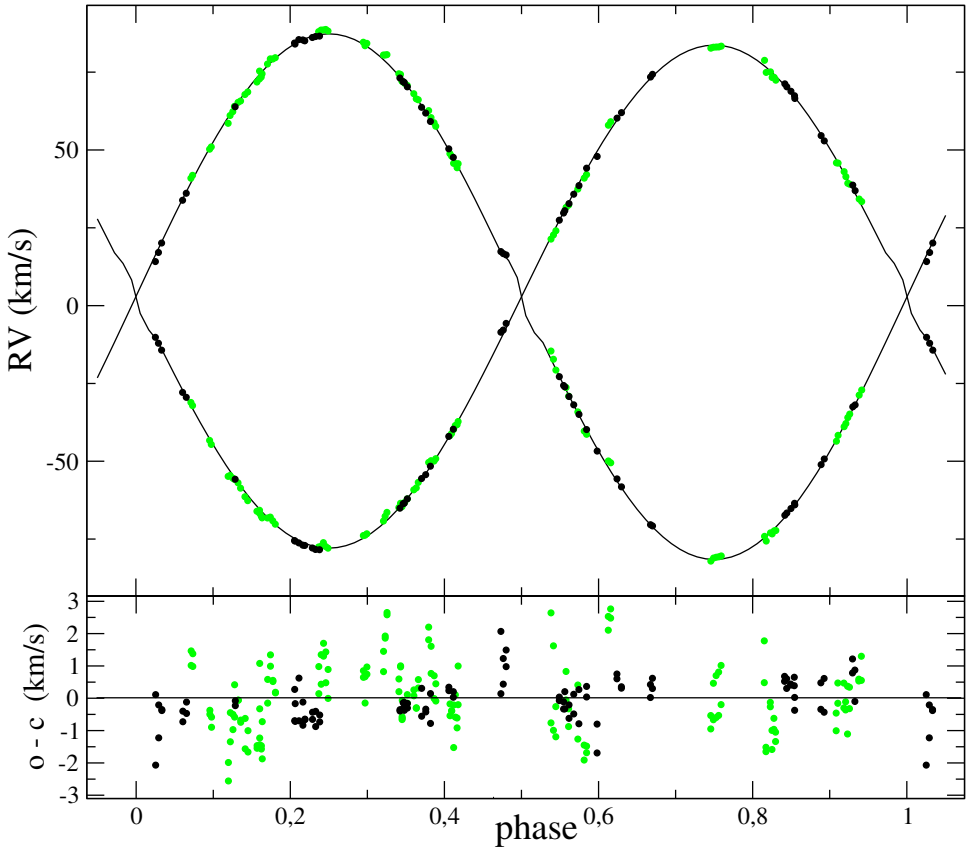

Fig. 5. Radial velocity curves of V2080 Cygni. Green dots represent DDO measurements shifted up by 1.1 $km\ s^{-1}$. Black dots represent measured PST1 velocities while the straight lines – synthetic RV curves based on the model listed in the one before last column of Table 3.

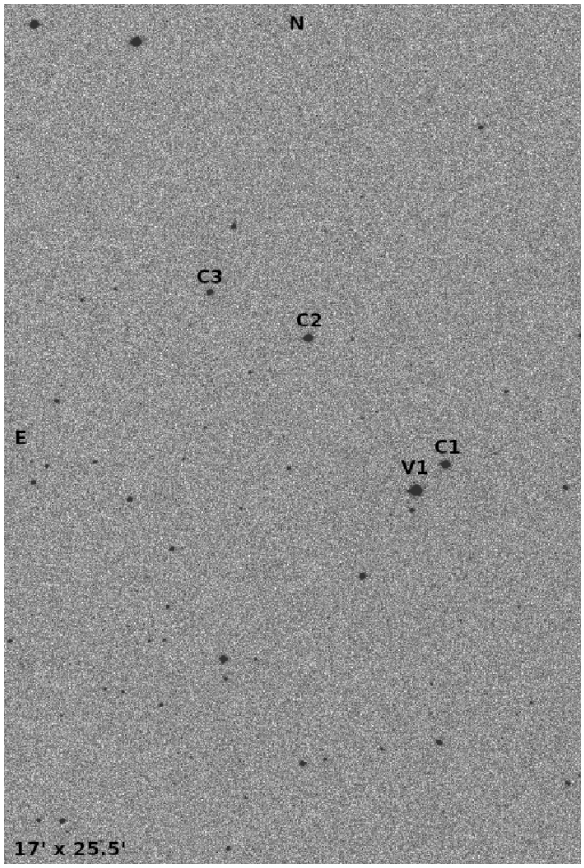

Fig. 6. Finding chart of V2080 Cyg. The variable is marked as V1. Positions of the three comparison stars C1, C2 and C3 are also shown. The field of view is about 17.0' $\times$ 25.5'. North is up, east is to the left.

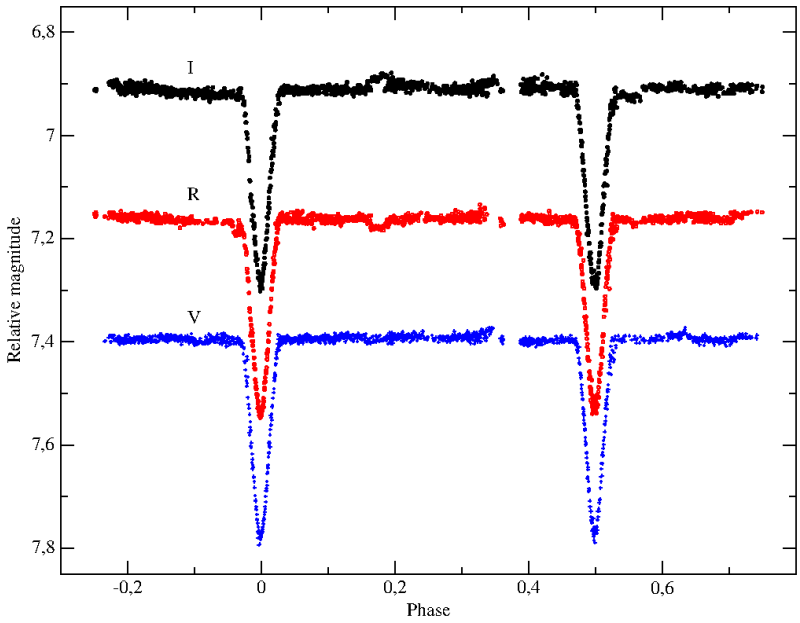

Fig. 7. The observed light curves in the I, R and V band passes for V2080 Cyg.

Dec$=+50^o09'18".274$, 8.56 mag in V filter), C2 (RA=$19^h27^m00^s.870$, Dec=$+50^o14'04".884$, 8.98 mag in V filter), and C3 (RA=$19^h27^m16^s.991$, Dec=$+50^o16'10".986$, 10.08 mag in V filter) were taken from the Tycho-2 Catalogue (Høg et al. 2000).

CCD frames were reduced with the *STARLINK*[4] package (Currie 2014). Corrections for bias, dark current and flat-field were applied and the aperture photometry was conducted.

In Fig. 7 we present the resulting light curves of V2080 Cygni in I, R and V filters. We used the value of 4.9335 days as an orbital period to phase the data.

5.2. $O-C$ diagrams for eclipses

To check the stability of the orbital period and determine its value, the $O-C$ analysis was conducted. First, we used the timings of 5 eclipses from our 2009-2011 observing season and the following ephemeris of the minima was derived:

$$\mathrm{HJD}_{\mathrm{min}} = 2455094.3114(2) + 4.933550(2) \times E, \qquad (1)$$

which gives the orbital period of $P_{orb1} = 4.933550(2)$ days. The resulting $O-C$ diagram for the moments of minima is shown in Fig. 8.

[4]The Starlink software is currently supported by the East Asian Observatory

Table 4: The journal of the CCD observations of V2080 Cyg.

Year	Start date	End date	Number of nights	Exposure time [sec]	Number of frames	Filter
2009	September 7	November 21	19	10	6306	V
				8	7248	I
				6	9550	R
2010	October 17	October 31	5	10	1726	V
				8	2141	I
				6	3012	R
2011	May 23	October 1	17	10	5515	V
				8	6888	I
				6	8313	R
Total:	-	-	41	-	50699	-

To obtain the best possible value of the orbital period we combined our 5 timings of eclipses from September 2009 - September 2011 observations, the SuperWASP[5] June-July 2008 data set, and the date presented in İbanoğlu et al. (2008). Based on this, we calculated the following ephemeris of the minima:

$$\mathrm{HJD}_{\mathrm{min}} = 2455094.31027(9) + 4.9335701(4) \times E, \quad (2)$$

and this corresponds to the orbital period of $P_{orb2} = 4.933701(4)$ days. In Fig. 9 we show the resulting $O-C$ diagram for the moments of eclipses for 1998-2011 time span.

In Table 5 we present the timings of eclipses with errors, cycle numbers E and $O-C$ values. As Type I and II are marked the primary and the secondary eclipses observed in V2080 Cyg, respectively.

The decreasing trend of the orbital period shown in Fig. 9 was confirmed by calculations of the second-order polynomial fit to the moments of minima. The following ephemeris was obtained:

$$\mathrm{HJD}_{\mathrm{min}} = 2455094.31054(9) + 4.9335634(6) \times E - 2.7(2) \times 10^{-8} \times E^2. \quad (3)$$

In Fig. 9 the solid line corresponds to the ephemeris given by Eq. 3.

After this investigation, we suggest that the orbital period might have not been stable between August 1998 and September 2011 and it can be described by a decreasing trend with a rate of $\dot{P} = -2.7(2) \times 10^{-8}$. It should be noted that the observed change in the orbital period, presented in Fig. 9, was calculated based on the only one point of data from 1998 given by İbanoğlu et al. (2008). Hence, this time span of observations and the amount of available data are insufficient for any conclusive statement pertaining to the changes in the orbital period of V2080 Cyg.

[5]https://wasp.cerit-sc.cz

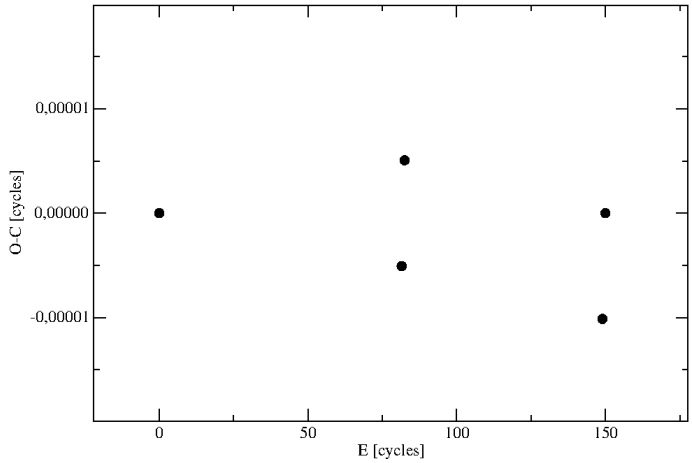

Fig. 8. The $O-C$ diagram of the moments of eclipses observed in V2080 Cyg during our 2009-2011 campaign.

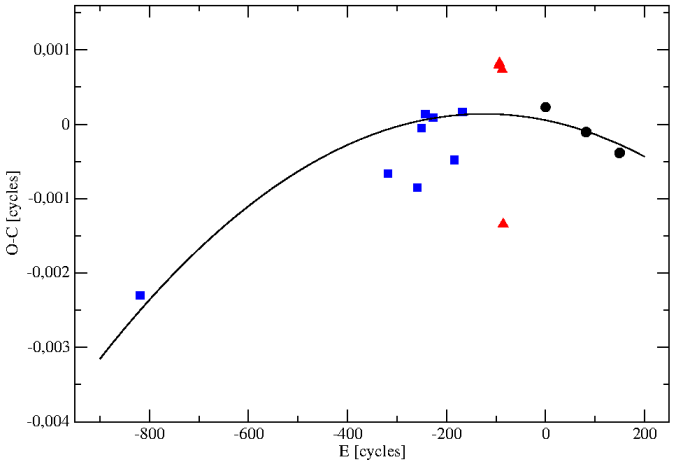

Fig. 9. The $O-C$ diagram of the moments of eclipses in V2080 Cyg based on data collected between 1998 and 2011 from both literature and our measurements. Black circles represent our dataset, data taken from the SuperWASP is marked with red triangles, and blue squares correspond to data provided by İbanoğlu et al. (2008).

Table 5: Times of minima in the light curves of V2080 Cyg observed since August 1998 until September 2011.

E	$\mathrm{HJD_{min}} - 2450000$	Error	$O-C$ [cycles]	Type	Reference
-819	1053.7050	-	-0.00230221	II	İbanoğlu et al. (2008)
-318	3525.4317	0.0008	-0.00066447	II	İbanoğlu et al. (2008)
-259	3816.5114	0.0006	-0.00085417	II	İbanoğlu et al. (2008)
-250.5	3858.4507	0.0003	-0.00005269	I	İbanoğlu et al. (2008)
-243	3895.4534	0.0001	0.00013467	II	İbanoğlu et al. (2008)
-227	3974.3903	0.0006	0.00089732	II	İbanoğlu et al. (2008)
-184	4186.5310	0.0003	-0.00048071	II	İbanoğlu et al. (2008)
-168	4265.4713	0.0006	0.00016353	II	İbanoğlu et al. (2008)
-94	4630.5586	0.0005	0.00079444	II	SuperWASP
-93	4635.4923	0.0008	0.00082077	II	SuperWASP
-87.5	4662.6265	0.0005	0.00073248	I	SuperWASP
-85.5	4672.4834	0.0006	-0.00134313	I	SuperWASP
0	5094.3114	0.0002	0.00022904	II	This work
81.5	5496.3957	0.0002	-0.00010807	I	This work
82.5	5501.3293	0.0003	-0.00010201	I	This work
149	5829.4103	0.0003	-0.00038814	II	This work
150	5834.3439	0.0004	-0.00038208	II	This work

6. Conclusions

The investigated object V2080 Cyg is a well detached system, which provides the posibility of precise measurements of absolute parameters. The star is bright and the spectral lines of both components are clearly resolved. The lines of both components are blended only near the eclipse phases. The binary has three relatively bright visual companions however GAIA proper motion and parallax results reveal that they are not connected with the EB as well as the dimmer background stars. We analysed our two radial velocity data sets obtaining a new mass determination based on a significantly higher number of measurements than the previous investigations. Comparing our and literature data we show that results depend on the usage of different instruments and different measurement methods. The influence of systematic errors on the obtained mass is about 1-2%. Additionally, we collected photometric data and calculated new times of minima. The analysis of eclipse times show possible variation of the orbital period, which must be confirmed with new measurements. Those variations could be related to a third body and the light-time effect in the system.

Acknowledgements. We would like to thank Slavek M. Rucinski and DDO staff for generous hospitality. In particular, our team wants to express appreciation to the observers Heide DeBond and Jim Thomson. We are grateful to our engineer Roman Baranowski the co-founder of the Poznań Spectroscopic Telescope project. We thank the people who helped in observations: Agata Rożek, Krystian Kurzawa, Anna Przybyszewska and Adrian Kruszewski. WD, TK, KK and ASC were supported by the Polish grant KBN 1 P03D 025 29.

This work has made use of data from the European Space Agency (ESA) mission *Gaia* (http://www.cosmos.esa.int/gaia), processed by the *Gaia* Data Processing and Analysis Consortium
(DPAC, http://www.cosmos.esa.int/web/gaia/dpac/consortium). Funding for the DPAC has been provided by national institutions, in particular the institutions participating in the *Gaia* Multilateral Agreement.

REFERENCES

Baranowski, R., Smolec, R., Dimitrov, W., et al. 2009, *MNRAS*, **396**, 4.
Currie, M. J., Berry, D. S., Jenness, T., et al. 2014, *ASPC*, **485**, 391C.
Dommanget, J., and Nys, O., 1994, *Communications de l'Observatoire Royal de Belgique*, **115**, .
Gaia Collaboration Brown, A. G. A., Vallenari, A., Prusti, T., de Bruijne, J. H. J., Mignard, F., et al. 2016, *A&A*, **special Gaia volume**, .
Høg, E., et al. 2000, *A&A*, **355L**, 27H.
İbanoğlu, C. et al. 2008, *MNRAS*, **384**, 1.
Kahraman Aliçavuş, F. and Aliçavuş, F. 2019, *MNRAS*, **488**, 4.
Kurpińska-Winiarska, M., Oblak, E., Winiarski, M. and Kundera, T. 2000, *IBVS*, **4823**, 1-3.
Lindegren, L., Lammers, U., Bastian, U., Hernández, J., Klioner, S., Hobbs, D., et al. 2016, *A&A*, **special Gaia volume**, .
Mason, B. D., Wycoff, G. L., Hartkopf, W. I., Douglass, G. G., and Worley, C. E., 2001, *AJ*, **122**, 3466.
Prša, A., and Zwitter, T., 2005, *ApJ*, **628**, 426.
Slavek Rucinski 1992, *AJ*, **104**, 1968R.
Slavek Rucinski 2002, *AJ*, **124**, 1746R.
Wilson, R. E., Devinney, E. J., 1971, *ApJ*, **166**, 605.